Radiology: Imaging Cancer

ORIGINAL RESEARCH

Development and Validation of Sorafenib-eluting Microspheres to Enhance Therapeutic Efficacy of Transcatheter Arterial Chemoembolization in a Rat Model of Hepatocellular Carcinoma

Wooram Park, PhD[1] • *Soojeong Cho, PhD* • *Jingran Ji, MD* • *Robert J. Lewandowski, MD* • *Andrew C. Larson, PhD* • *Dong-Hyun Kim, PhD*

From the Department of Radiology, Feinberg School of Medicine (W.P., S.C., J.J., R.J.L., A.C.L., D.H.K.), and Robert H. Lurie Comprehensive Cancer Center (R.J.L., A.C.L., D.H.K.), Northwestern University, 737 N Michigan Ave, Suite 1600, Chicago, IL 60611; Department of Biomedical Engineering (A.C.L., D.H.K.); and Department of Electrical Engineering and Computer Science (A.C.L.) and International Institute of Nanotechnology (A.C.L.), Northwestern University, Evanston, Ill. Received January 28, 2020; revision requested March 25; revision received September 4; accepted September 15. **Address correspondence to** D.H.K. (e-mail: *dhkim@northwestern.edu*).

Current address:

[1]Department of Biomedical-Chemical Engineering, The Catholic University of Korea, Bucheon, Republic of Korea

Supported by Guerbet, the National Institutes of Health (grants R01CA181658, R01CA218659, and R01EB026207), and the Center for Translational Imaging and Mouse Histology and Phenotyping Laboratory at Northwestern University

Conflicts of interest are listed at the end of this article.

See also the commentary by Yamada and Gayed in this issue.

Radiology: Imaging Cancer 2021; 3(1):e200006 • https://doi.org/10.1148/rycan.2021200006 • Content codes: GI MR OI

Purpose: To validate the therapeutic efficacy of sorafenib-eluting embolic microspheres (SOR-EMs) used in combination with transarterial chemoembolization (TACE) for treatment of hepatocellular carcinoma (HCC) in a preclinical animal model.

Materials and Methods: SOR-EMs were prepared with poly(D,L-lactide-*co*-glycolide), iron oxide nanoparticles, and sorafenib. The morphology of the prepared SOR-EMs was confirmed by using optical microscopy. Drug release from the SOR-EMs was quantified in vitro by using high-performance liquid chromatography. In an orthotopic rat model of HCC, embolic doxorubicin–Lipiodol (ethiodized oil) emulsion (DLE) and SOR-EMs were sequentially injected into the hepatic artery of the rats: The rats in group 1 were injected with DLE; group 2 was injected with DLE plus unloaded embolic microspheres (DLE + EM); group 3, with DLE plus SOR-EMs (DLE + SOR-EM); and group 4, with saline solution. The SOR-EM and tumor size changes in each group (of six rats each) over time were measured by using MRI. Tissues were assessed by using immunohistochemistry, with hematoxylin-eosin and terminal deoxynucleotidyl transferase-mediated dUTP (2'-deoxyuridine 5'-triphosphate) nick-end labeling staining used for dead cells and CD34 staining used for new microvessel formation.

Results: The SOR-EMs were a mean size of 6.6 μm ± 2.3 (standard deviation) and showed 53.7% ± 8.3 sorafenib loading efficiency with T2-weighted MRI capability. In the HCC rat model, the intra-arterially injected SOR-EMs were successfully monitored by using MRI. The DLE + SOR-EM–treated rats showed a superior tumor growth–inhibitory effect compared with the rats treated with DLE only ($P < .05$). Immunohistochemical assessment of tissue specimens showed that compared with the other treatment groups, the DLE + SOR-EM treatment group had the lowest number of microvessels, as quantified by using the percentage of CD34-positive stained area ($P < .01$ for all comparisons).

Conclusion: In a preclinical rat HCC model, SOR-EMs used in combination with DLE TACE were effective in treating HCC.

Supplemental material is available for this article.

© RSNA, 2021

Transcatheter arterial chemoembolization (TACE) typically involves the transcatheter hepatic arterial administration of chemotherapeutic drugs (eg, doxorubicin) emulsified in ethiodized oil (Lipiodol; Guerbet, Villepinte, France) (1–3), which is immediately followed by the administration of embolic materials. The immediate administration of embolic materials is intended to transiently halt forward flow to slow drug washout rates and consequently extend tumor tissue exposure to the drugs released from the previously infused emulsion. With ethiodized oil TACE, the immediate administration of embolic materials has the potential to cause hypoxic conditions within the treated areas (4), which may induce angiogenesis to reestablish blood flow, potentially allowing portions of the tumor to survive. An increase in serum vascular endothelial growth factor (VEGF) levels the first day after TACE has been correlated to poorer patient outcomes, and elevated VEGF levels have been observed for up to a month after therapy (5,6). Rather than the use of current bland (unloaded) embolization microspheres or embolic particles to halt the forward flow of blood during ethiodized oil TACE procedures, we propose the development and preclinical validation of drug-eluting embolic microspheres that locally deliver antiproliferation and antiangiogenic agents to prevent the phenomenon of hypoxia-induced angiogenesis.

This copy is for personal use only. To order printed copies, contact reprints@rsna.org

Abbreviations

DLE = doxorubicin-Lipiodol emulsion, HCC = hepatocellular carcinoma, PLGA = poly (D,L-lactide-*co*-glycolide), SOR-EM = sorafenib-eluting embolic microspheres, TACE = transarterial chemoembolization, TUNEL = terminal deoxynucleotidyl transferase-mediated dUTP (2'-deoxyuridine 5'-triphosphate) nick-end labeling, VEGF = vascular endothelial growth factor

Summary

Sorafenib-eluting embolic microspheres that could be imaged with MRI, in combination with transcatheter arterial chemoembolization, were effective in treating hepatocellular carcinoma through inhibition of angiogenesis in a preclinical animal model.

Key Points

- Rats treated with combined doxorubicin–Lipiodol (iodized oil) emulsion (DLE) transcatheter arterial chemoembolization (TACE) and sorafenib-eluting embolic microspheres (SOR-EMs) showed a superior tumor growth–inhibitory effect compared with rats treated with DLE TACE ($P = .008$).
- Immunohistochemical assessment of tumor tissues showed that the development of new microvessels was reduced in the DLE–SOR-EM TACE group compared with the DLE TACE group ($P < .001$).
- A combination of TACE and SOR-EMs has therapeutic potential for the treatment of hepatocellular carcinoma.

Sorafenib tosylate is a potent multikinase inhibitor that was approved in 2008 for the treatment of patients with unresectable hepatocellular carcinoma (HCC) (7,8). Sorafenib inhibits angiogenesis by means of targeted blockage of VEGF and platelet-derived growth factor receptors and inhibits cell proliferation by blocking B-Raf proto-oncogene serine/threonine-protein kinase and RAF proto-oncogene serine/threonine-protein kinase in the mitogen-activated protein kinase pathway (9,10). In this study, we combined TACE with local administration of sorafenib to inhibit both revascularization and tumor proliferation. We hypothesized that the concurrent targeted delivery of sorafenib multikinase inhibitors via drug-eluting microspheres during TACE would enhance therapeutic efficacy, which we assessed in a preclinical HCC rat model.

Materials and Methods

Study Design

Experiments were supported by a research grant from Guerbet. In vivo studies were performed with approval from the Institutional Animal Care and Use Committee at Northwestern University. N1S1 hepatoma cells (1×10^6 cells) were suspended in Dulbecco's modified Eagle's medium and directly implanted in the left lateral liver lobe in 24 male Sprague-Dawley 12-week-old rats by using mini-laparotomy procedures (11). Tumors were allowed to grow for 7 days to reach a size of approximately 5 mm in diameter while the animals were observed daily for any signs of distress (ie, weight loss, decreased food and water consumption, and dehydration). The rats were separated into four treatment groups, with six rats in each group. The number of animals per group was determined by reference to previous studies (12–14). Group 1 consisted of rats that received intra-arterial transcatheter administration of the doxorubicin–Lipiodol (ethiodized oil) emulsion (DLE); group 2, rats that received DLE and unloaded embolic microspheres (DLE + EM); group 3, rats that received DLE and embolic microspheres loaded with sorafenib (DLE + SOR-EM); and group 4 (control), rats injected with saline solution.

Reagents and Solvents

All reagents and solvents were obtained commercially and used without further purification. Poly(D,L-lactide-*co*-glycolide) (PLGA) (lactide-glycolide ratio, 50:50), polyvinyl alcohol (molecular weight, 89−98 kDa [>99% hydrolyzed]), iron(III) chloride hexahydrate (≥98%), dichloromethane, chloroform, dimethyl sulfoxide, methanol, *n*-docosane (99%), 1-octadecene (90%), *n*-hexane, and ethanol were purchased from Sigma-Aldrich (Milwaukee, Wis). Sodium oleate (>97%) was purchased from TCI America (Portland, Ore). Sorafenib tosylate was purchased from LC Laboratories (Woburn, Mass).

Synthesis of Iron Oxide Nanoparticles

Iron oxide nanoparticles were prepared by using the thermal decomposition method (15,16). Before the synthesis of nanoparticles, iron oleate was synthesized by using a previously described method (17). Iron oleate (1.57 g), *n*-docosane (6.0 g), and sodium oleate (0.53 g) were mixed in 11 mL of 1-octadecene and reacted at 120°C for 1 hour. The solution was then heated to 337°C at a rate of 3°C per minute by using a digital temperature controller (Cole-Parmer, Vernon Hills, Ill) and stirred for 30 minutes. The synthesized nanoparticles were purified by means of centrifugation and washed with *n*-hexane three times. Finally, the nanoparticles were air dried at room temperature and redispersed in chloroform.

Preparation of SOR-EMs

SOR-EMs were prepared by using the emulsion and solvent evaporation method. PLGA (100 mg) was dissolved in 4 mL of dichloromethane and then combined with 20 mg of sorafenib that was dissolved in 200 μL of dimethyl sulfoxide and 1 mg of iron oxide nanoparticles dissolved in 100 μL of dichloromethane. The solution was mixed by means of vigorous vortexing for 1 minute. This first emulsion was further injected into an aqueous solution containing 2-wt% polyvinyl alcohol to form an emulsion, and the emulsification process was performed by using a homogenizer at 2000 revolutions per minute for 5 minutes. The organic solvent in the emulsion was evaporated for 12 hours by means of overhead stirring (200 revolutions per minute) at room temperature. The PLGA microspheres were collected after 5 minutes of centrifugation at 3000 revolutions per minute and then washed three times with deionized water. The resulting samples were lyophilized and stored at −20°C. The morphologic characteristics and size distribution of the samples were determined by using scanning electron microscopy (Hitachi S-4800; Hitachi, Tokyo, Japan).

R2-Mapping Image of Agar Phantoms with SOR-EMs

R2-mapping images of agar phantoms with SOR-EM were taken by using a 7-T MRI unit (BioSpec; Bruker, Billerica, Mass). Imaging phantoms were prepared by using 1% agar at various concentrations of SOR-EMs (0-19 mg/mL) in a 1.5-mL Eppendorf tube. The MRI sequence for the phantom study was used according to the protocol followed in our previous study (18,19).

Preparation of DLE

To prepare the DLE, 6 mg of doxorubicin (LC Laboratories; Woburn, Mass) in 0.5 mL of phosphate-buffered saline was mixed with 0.5 mL of ethiodized oil (Lipiodol). Emulsions composed of doxorubicin solution (aqueous phase) and ethiodized oil (oil phase) were prepared by means of repetitive pumping through a three-way stopcock.

Sorafenib Release Studies

The sorafenib release test was performed by following the protocol used in our previous study (20). SOR-EMs were incubated in 5 mL of release medium containing 10 mM (10 mmol/L) of phosphate-buffered saline (pH, 7.4; 0.02-wt% polyoxyethylene sorbitan monooleate [Tween 80; Sigma-Aldrich]). The temperature of the water-bath incubator was maintained at 37°C, with continuous agitation at 50 revolutions per minute. At each sampling time, the supernatant of release medium was removed after 5 minutes of centrifugation at 3000 revolutions per minute and replaced with fresh medium. The amount of released sorafenib was determined by using reverse-phase high-performance liquid chromatographic analysis performed under previously described conditions (21).

Characterization of Iron Oxide Nanoparticles Loaded in SOR-EMs

The iron oxide nanoparticle content in the SOR-EMs was characterized by using inductively coupled plasma mass spectrometry (PerkinElmer; Waltham, Mass). In triplicate, SOR-EMs (10 mg) were digested in 200 μL of nitric acid (70%) at 60°C and diluted to 5 mL of a 2% nitric acid solution, with 5-ppb yttrium used as an internal standard.

Catheterization and TACE Procedures

Procedures to invasively catheterize the proper hepatic artery were performed in all of the rats, as described previously (19,22,23). TACE procedures were performed 7 days after N1S1 cell implantation. The catheterization procedure involved laparotomy and subsequent isolation of the portal triad above the first loop of the duodenum. The common hepatic artery was clamped with a vascular clamp to temporarily prevent blood flow through the hepatic gastroduodenal arteries while the catheter was inserted. A 4-0 suture was used to permanently ligate the gastroduodenal artery to prevent retrograde flow of the samples to the bowels during administration through the catheter. A 1.5-Fr microcatheter (Marathon; EV3, Irvine, Calif) was inserted distally to the ligated 4-0 suture in the gastroduodenal artery and then guided into the proper hepatic artery from the gastroduodenal artery. X-ray digital subtraction angiography with use of an iodinated contrast agent (iohexol [Omnipaque; Amersham, Little Chalfont, England]) was performed to confirm catheter placement in the common branch of the proper hepatic artery (23). The rats received a single subcutaneous injection of buprenorphine (0.01–0.05 mg/kg), followed by meloxicam (1–2 mg/kg). Meloxicam was administered every 24 hours for a minimum of 2 days after surgery.

For the group 1 (DLE), group 2 (DLE + EM), and group 3 (DLE + SOR-EM) rats, a 0.1-mL dose of DLE, equivalent to a 1-mg/kg dose of doxorubicin, was injected. In TACE, the recommended dose of doxorubicin and ethiodized oil is less than or equal to 2 mg/kg for human adults (24). For groups 2 and 3, follow-up embolization was performed by administering 20-mg doses of either unloaded embolic microspheres or SOR-EMs to achieve near-stasis conditions in each animal. Note that a 20-mg SOR-EM dose is equivalent to a 5-mg/kg dose of sorafenib, which is the recommended daily dose in patients with HCC (25). A 0.2-mL saline flush was then infused before the catheter was withdrawn; the group 4 (control) rats received only this 0.2-mL saline flush. At completion of the intra-arterial administration procedures, the gastroduodenal artery was ligated above the insertion position to prevent bleeding out through the catheter insertion point prior to removal and closure of the abdomen for recovery. Following the interventional procedures, each rat was examined with MRI.

In Vivo MRI

T2-weighted MR images were collected prior to catheterization and after intra-arterial administration of the DLE and EMs. MRI was performed with a 7-T MRI unit (BioSpec) in both coronal and axial orientations by using a turbo spin-echo sequence and the following parameters: repetition time, 2000 msec; echo time, 30 msec; 1-mm section thickness; field of view, 71 × 85 mm; 216 × 256 matrix; and respiratory triggering with an MRI-compatible small animal gating system (model 1025; SA Instruments, Stony Brook, NY). MRI measurements were then repeated 7 and 14 days after treatment.

Tumor Size Measurement

Tumor size was measured, as previously described (20). The width and length of the tumors were measured by using MRI at baseline and 7 and 14 days after treatment. The tumor volume was calculated by using the formula $V = (a^2 \times b)/2$, where V is the tumor volume, a is the width, b is the length, and a is less than or equal to b. For comparison, the tumor volume was normalized by its initial volume: V/V_0, where V_0 is the volume of the tumor at the time of therapy.

Histologic Characteristics and Immunohistochemistry

To confirm antitumor therapeutic efficacy, livers were harvested from the rats 2 weeks after each treatment in experi-

mental groups, and the tumor-containing segments were resected for microtome sectioning. Five-micrometer slices through the center of each tumor were used for hematoxylin-eosin, terminal deoxynucleotidyl transferase-mediated dUTP (2′-deoxyuridine 5′-triphosphate) nick-end labeling (TUNEL), and rat anti-CD34 staining, as previously described (18,20). All slides were analyzed by using a TissueFAXS microscope (TissueGnostics; Vienna, Austria). Quantitative analyses of tumor necrosis (with hematoxylin-eosin staining) and tumor angiogenesis (with CD34 immunohistochemical staining) were performed by using Image J software (National Institutes of Health; Bethesda, Md). Following the protocol described in a previous report (19), tumor microvessel density was expressed as the ratio of the CD34-positive stained area to the total tumor area.

Statistical Analysis

Tumor growth and TUNEL- and CD34-stained tissue from each rat group were statistically analyzed to validate our hypothesis that a combination of TACE and DLE plus SOR-EMs (DLE + SOR-EM) would show better treatment efficiency for HCC than would conventional TACE. The statistical significance of differences between the two TACE groups was determined by using the Student unpaired *t* test. $P < .05$ was considered to indicate a significant difference. All statistical analyses were performed by using GraphPad Prism 6.0 software (GraphPad Software; La Jolla, Calif).

Results

Preparation and Characterization of SOR-EMs

We used a single emulsion method to prepare biodegradable drug-eluting microspheres that included iron oxide, enabling the use of MRI for confirmation of delivery to the targeted tumors. The synthesized iron oxide nanoparticles were uniformly cube shaped at transmission electron microscopy (Fig 1, *A*). The mean size of the spherical SOR-EMs (Fig 1, *B*) was 6.6 μm ± 2.3 (standard deviation) (Fig 1, *C*). As shown in the Table, the mean contents of iron oxide nanoparticles and sorafenib in total mass were 0.23 wt% ± 0.1 and 10.7 wt% ± 1.7, respectively. The characteristics of the prepared SOR-EMs (eg, size and morphology) were similar to those in a previous report (20). Although rapid drug release (up to approximately 40%) occurred during the initial observation period (<5 hours), the drug release then slowed considerably over the remaining 100 hours of observation, as quantified by using high-performance liquid chromatography (Fig 1, *D*).

In Vitro and in Vivo Evaluation of MRI for SOR-EM Visualization

We performed R2-mapping 7-T MRI by using phantom vials with increasing microsphere concentrations to confirm the capability to use MRI for visualization of the SOR-EMs. As shown in Figure 1, *E*, the R2 signal intensity gradually decreased with increasing concentration of SOR-EMs, suggesting the feasibility of using MRI to confirm microsphere delivery. As shown in Figure 2, the T2-weighted MRI intensity at the periphery of tumors decreased after administration of the SOR-EMs, suggesting deposition of the iron oxide–containing microspheres within the well-vascularized peripheral regions (as opposed to the central core of N1S1 tumors, which are poorly vascularized). Although some signal intensity changes were observed in normal liver tissue, as seen in Figure 2, no liver toxicity was observed.

In Vivo Evaluation for Tumor Growth Inhibition

The tumor growth in each rat group was monitored with MRI for 2 weeks. After 2 weeks, the mean tumor size for the group treated with DLE + SOR-EM was smaller than that for the other groups ($P < .001$ [control], $P = .008$ [DLE], and $P = .03$ [DLE + EM]) (Fig 3). Actual tumor volume changes are provided in Table E1 (supplement). Finally, representative tumor tissue specimens were collected from each group for histologic analysis. As shown in Figure 4, apoptosis of tumor cells (TUNEL stain positive) was highest in the rats treated with DLE + SOR-EM (62.69% ± 5.95 [mean ± standard deviation]) compared with the apoptosis in the control (0.34% ± 0.09; $P < .001$), DLE-treated (38.95% ± 7.25; $P = .002$), and DLE + EM–treated (31.52% ± 4.49; $P < .001$) groups (Fig 5, *A*, Table E2 [supplement]). Consistent with these results, the findings in representative specimens confirmed that microvessel density, as measured according to CD34-positive areas, was reduced in the DLE + SOR-EM–treated tumors (0.30% ± 0.19) compared with the tumors in the control group rats (1.81% ± 0.41; $P < .001$), rats treated with DLE (3.42% ± 0.64; $P < .001$), and rats treated with DLE + EM (4.82% ± 0.73; $P < .001$) (Fig 5, *B*, Table E2 [supplement]). No morphologic changes in the liver were observed between groups after the TACE procedures.

Discussion

The SOR-EMs were successfully synthesized by using a single emulsion method. In the HCC rat model, the group treated with intra-arterially administered DLE and immediate–follow-up embolization with SOR-EMs demonstrated a reduction in tumor growth compared with the DLE, DLE + EM, and control (saline injection) groups ($P < .05$ for all comparisons). Results of immunohistochemical analysis suggested that tumor angiogenesis was suppressed and apoptotic cell death increased when tumors were treated with the combination of DLE embolization and SOR-EMs. These study results validate the combination treatment effect of functional embolic microspheres encapsulating multikinase inhibitor, iron oxide nanoparticles, and TACE with use of ethiodized oil and doxorubicin in a preclinical HCC model.

In recent phase-III clinical trials (26), the combination of TACE plus sorafenib did not show a satisfactory benefit in terms of progression-free survival compared with TACE alone. Investigators in past clinical studies adopted oral administration of sorafenib for patients with intermediate-stage HCC after TACE. In this study, however, sorafenib

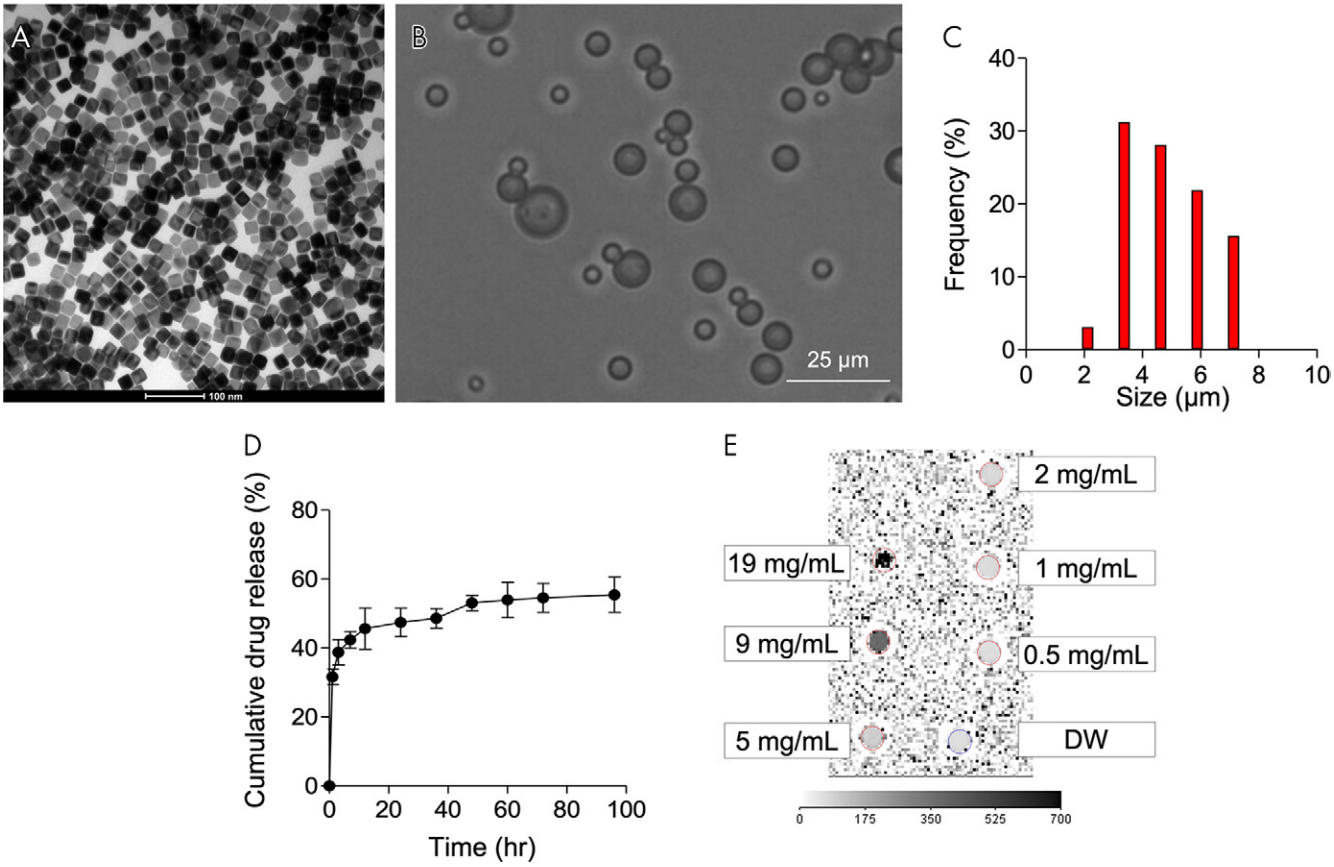

Figure 1: Characterization of sorafenib-eluting embolic microspheres (SOR-EMs). *A*, Transmission electron microscopy image of iron oxide nanoparticles (scale bar, 100 nm). *B*, Optical microscopy image of SOR-EMs (scale bar, 25 μm); color was converted to gray. *C*, Graph shows the size distribution of SOR-EMs. *D*, Graph shows cumulative measurements of in vitro drug release from SOR-EMs in phosphate-buffered saline (150 mM [150 mmol/L]; pH, 7.4) at 37°C in the three TACE groups. *E*, R2-mapping MR image of 1% agar phantoms shows increasing concentrations (in milligrams per milliliter) of SOR-EMs at 7-T MRI. DW = distilled water.

Characterization of SOR-EMs

Sample	Feed IONPs (mg)*	Feed Sorafenib (mg)†	IONP Loading Efficiency (%)‡	IONP Content (wt%)‡	Sorafenib Loading Efficiency (%)§	Sorafenib Content (wt%)§
SOR-EMs	1.25	20	18.6 ± 5.9	0.23 ± 0.1	53.7 ± 8.3	10.7 ± 1.7

Note.—IONP = iron oxide nanoparticle, SOR-EMs = sorafenib-eluting embolic microspheres.
*Weight of IONP per 100 mg of poly(lactide-co-glycolide).
†Weight of sorafenib per 100 mg of poly(lactide-co-glycolide) included in the synthesis procedure.
‡Encapsulation efficiency = (actual mass of IONPs or sorafenib/feed mass of IONPs or sorafenib) × 100, as determined at inductively coupled plasma optical emission spectrometry. Datum is the mean value ± standard deviation.
§Loading contents = (mass of IONPs or sorafenib/total mass of SOR-EM) × 100, as determined at high-performance liquid chromatography (in three TACE groups). Datum is the mean value ± standard deviation.

was encapsulated in biodegradable microspheres and delivered locally to the tumor site after TACE. This strategy facilitated more effective inhibition of tumor growth owing to a concentrated amount of the drug at the tumor site.

Preclinical studies involving the use of only SOR-EMs for treatment of HCC have been published (18–20), and in the current work we expanded on previous studies by assessing a combination of TACE and SOR-EMs. DLE-based TACE has been an interventional chemotherapy for the treatment of patients with HCC for more than 30 years (27–29). Thus, preclinical studies of TACE in combination with DLE and SOR-EMs could be an important basis for developing more effective HCC treatments. Although recent studies (30,31) have shown that emulsions with a high ethiodized oil ratio have high stability, the 1:1 ratio of doxorubicin and ethiodized oil is still widely used in the clinical setting. In future studies, high ethiodized oil ratios also will need to be tested.

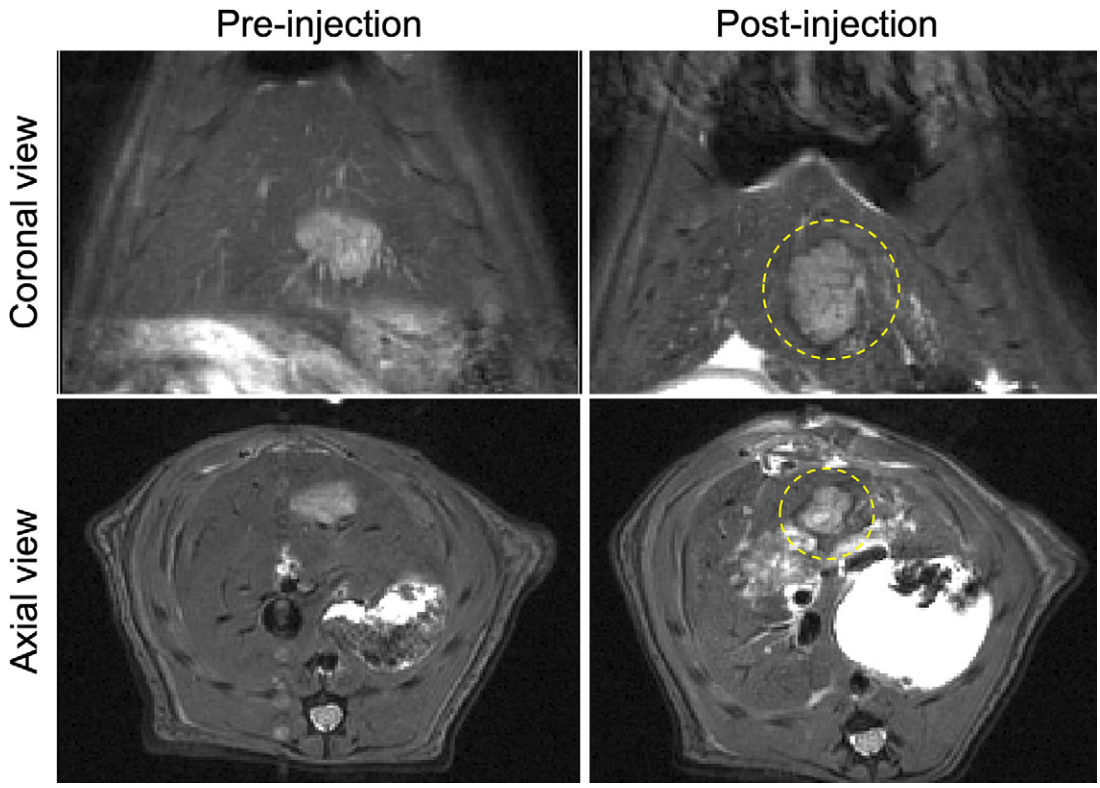

Figure 2: MR images obtained before and after the injection of sorafenib-eluting embolic microspheres (SOR-EMs) into the hepatic artery. Dotted circles outline regions of marked T2-weighted signal intensity changes caused by the deposition of iron oxide–labeled SOR-EMs at the typical hypervascular periphery of the tumor.

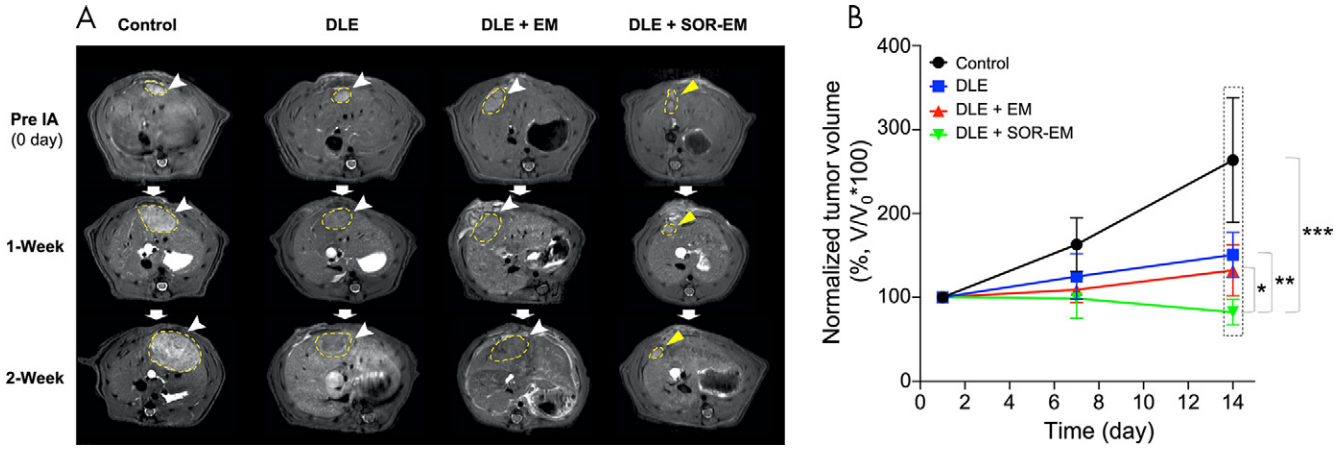

Figure 3: In vivo tumor growth inhibition after transcatheter arterial chemoembolization (TACE). *A*, In vivo MR images show tumor growth (dotted outlines, arrowheads) observed over time. IA = intra-arterial injection. *B*, Graph shows changes in normalized tumor volume (V) as a function of time after administration of doxorubicin-Lipiodol emulsion (DLE) plus sorafenib-eluting microspheres (DLE + SOR-EM) (six rats per group, three treatment groups; **P* < .001, ***P* = .008, and ****P* = .03). DLE + EM = DLE plus unloaded embolic microspheres, V_0 = tumor volume at the time of therapy.

SOR-EMs encapsulated with iron oxide nanoparticles are cube shaped and can be monitored in vivo with high sensitivity by using MRI. Although the embolic microspheres used in TACE procedures for humans are larger than 100 μm (32), the SOR-EMs used in this study were smaller than 10 μm to allow studies in rat arteries (~650 μm). In general, PLGA microspheres release the encapsulated drug during bulk erosion (33). SOR-EMs exhibited a fast initial release rate. The release rate can be controlled by selecting PLGA polymers with appropriate degradation rates.

In this study, N1S1 hepatoma cells were transplanted in rat livers to create a preclinical orthotopic HCC model. Although prior study investigators have reported that the N1S1 model exhibits a spontaneous decrease in tumor size (34), no spontaneous reduction in tumor size was observed in our N1S1 model, which was generated with surgical cell implantation. MR image findings indicated that our SOR-EMs can be traced in vivo by using MRI. This finding is consistent with previous research (20,35). Although the SOR-EMs had a

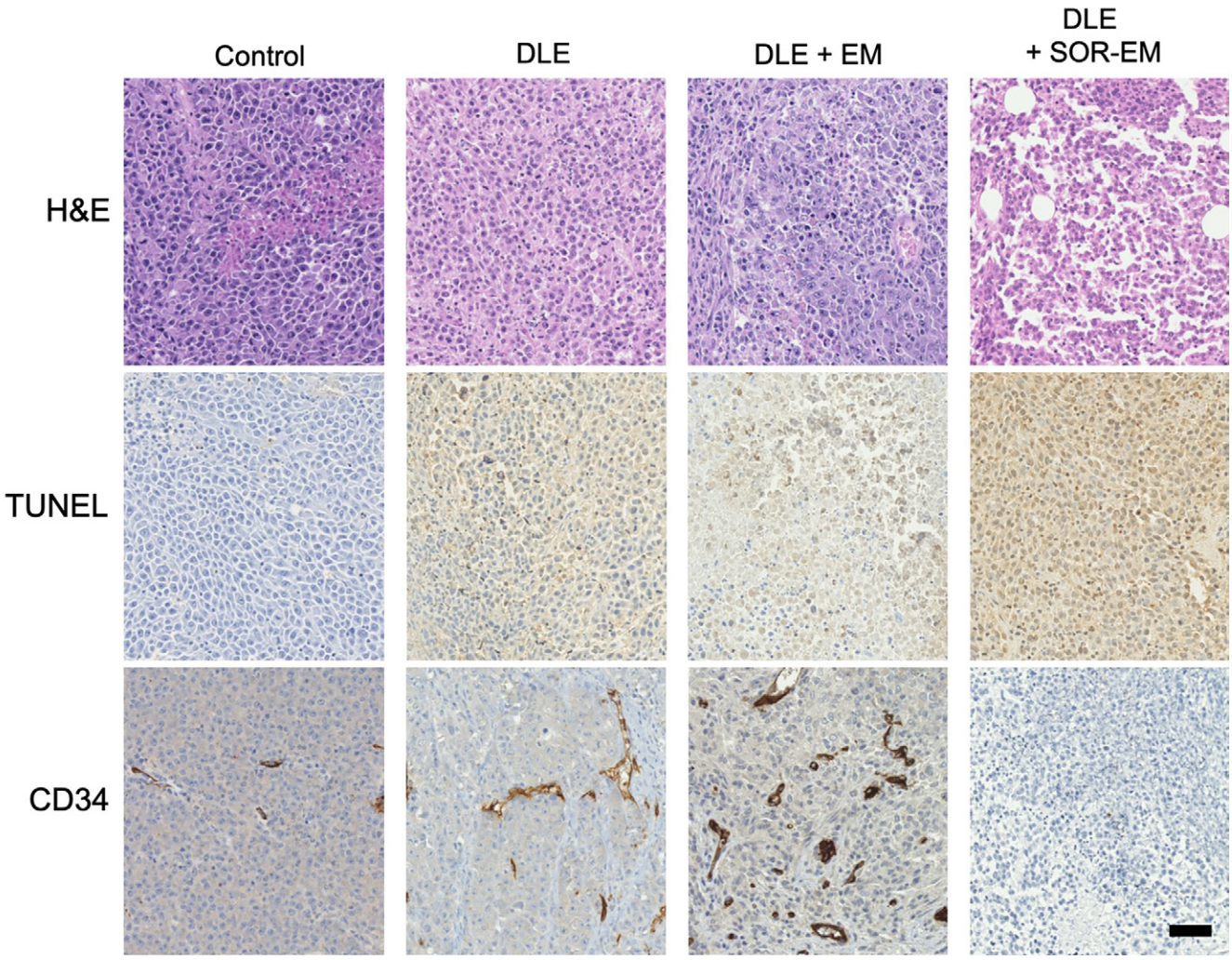

Figure 4: Histologic and immunohistochemical analyses of tumor tissue 2 weeks after TACE treatments. Tumor tissue specimens stained with hematoxylin-eosin (H&E), terminal deoxynucleotidyl transferase-mediated dUTP (2′-deoxyuridine 5′-triphosphate) nick-end labeling (TUNEL) stain, and human progenitor cell antigen (CD34) are shown. Brown color on the TUNEL- and CD34-stained tissue indicates TUNEL-positive apoptotic cells (TUNEL-stained specimens) and microvessels (on CD34-stained specimens) (scale bar, 25 μm). DLE = doxorubicin–Lipiodol emulsion, DLE + EM = DLE plus embolic microspheres, DLE + SOR-EM = DLE plus sorafenib-eluting EMs.

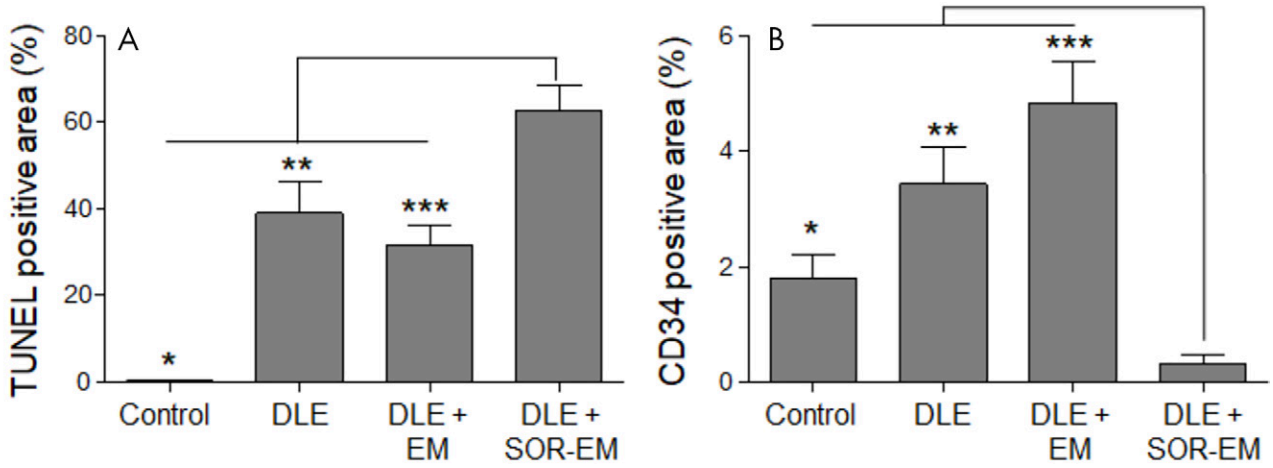

Figure 5: *A, B,* Quantitative analysis of, *A,* terminal deoxynucleotidyl transferase-mediated dUTP (2′-deoxyuridine 5′-triphosphate) nick-end labeling (TUNEL)-positive (*$P < .001$, ** = .002, ***$P < .001$) and, *B,* human progenitor cell antigen (CD34)-positive areas (*$P < .001$, **$P < .001$, ***$P < .001$) in tumor tissue analyzed 2 weeks after the TACE treatment procedures (four rats per group). DLE = doxorubicin-Lipiodol emulsion, DLE + EM = DLE plus embolic microspheres, DLE + SOR-EM = DLE plus sorafenib-eluting EMs.

particle size similar to that of red blood cells, they accumulated only around the tumor. This phenomenon is presumed to be due to low tissue permeability, because red blood cells are composed of flexible lipid membranes, whereas SOR-EMs are made of rigid biopolymers. However, the SOR-EMs could not be monitored by using MRI at 7 and 14 days after the injection. This is presumably because the PLGA (50:50 lactide-glycolide ratio) constituting the SOR-EMs has a fast decomposition time of within several weeks (36).

Our animal study had several limitations. First, the tumor responses in each group were examined with a small number of rats. Second, we did not evaluate adverse effects, such as lung embolism and hepatotoxicity, that may occur with use of TACE and SOR-EMs. Although no detailed hepatotoxicity studies were conducted in this study, we plan to evaluate liver enzymes in future research. Third, the effects of the particle size and dose of SOR-EMs on the treatment of HCC were not investigated.

Compared with the control group, the group treated with traditional TACE with use of DLE exhibited an anticancer therapeutic effect; however, the best tumor-suppression effect was observed in the DLE + SOR-EM–treated group. Tumor tissues were assessed for expression of CD34, an angiogenic marker, and it was found that the group injected with DLE + SOR-EM had lower CD34-positive areas than did the other groups. Together, these results suggest that the use of TACE combined with SOR-EMs can inhibit the growth of HCC by reducing angiogenesis, which is induced by hypoxic conditions after TACE. Although the combination treatment of SOR-EMs and TACE requires further verification of long-term therapeutic efficacy and safety, the results of this study show that SOR-EMs in combination with TACE have potential for effective HCC treatment.

Author contributions: Guarantors of integrity of entire study, W.P., D.H.K.; study concepts/study design or data acquisition or data analysis/interpretation, all authors; manuscript drafting or manuscript revision for important intellectual content, all authors; approval of final version of submitted manuscript, all authors; agrees to ensure any questions related to the work are appropriately resolved, all authors; literature research, W.P., R.J.L., D.H.K.; experimental studies, all authors; statistical analysis, W.P., S.C., D.H.K.; and manuscript editing, W.P., J.J., R.J.L., A.C.L., D.H.K.

Disclosures of Conflicts of Interest: **W.P.** disclosed no relevant relationships. **S.C.** disclosed no relevant relationships. **J.J.** disclosed no relevant relationships. **R.J.L.** disclosed no relevant relationships. **A.C.L.** Activities related to the present article: institutional grant (1R01CA181658) from National Institutes of Health. Activities not related to the present article: disclosed no relevant relationships. Other relationships: disclosed no relevant relationships. **D.H.K.** disclosed no relevant relationships.

References

1. Geschwind JF, Ramsey DE, Choti MA, Thuluvath PJ, Huncharek MS. Chemoembolization of hepatocellular carcinoma: results of a metaanalysis. Am J Clin Oncol 2003;26(4):344–349.
2. Llovet JM, Bruix J. Systematic review of randomized trials for unresectable hepatocellular carcinoma: chemoembolization improves survival. Hepatology 2003;37(2):429–442.
3. Lo CM, Ngan H, Tso WK, et al. Randomized controlled trial of transarterial lipiodol chemoembolization for unresectable hepatocellular carcinoma. Hepatology 2002;35(5):1164–1171.
4. Johnson CG, Sharma KV, Levy EB, et al. Microvascular perfusion changes following transarterial hepatic tumor embolization. J Vasc Interv Radiol 2016;27(1):133–141.e3.
5. Jia ZZ, Jiang GM, Feng YL. Serum HIF-1α and VEGF levels pre- and post-TACE in patients with primary liver cancer. Chin Med Sci J 2011;26(3):158–162.
6. Li X, Feng GS, Zheng CS, Zhuo CK, Liu X. Expression of plasma vascular endothelial growth factor in patients with hepatocellular carcinoma and effect of transcatheter arterial chemoembolization therapy on plasma vascular endothelial growth factor level. World J Gastroenterol 2004;10(19):2878–2882.
7. Llovet JM, Ricci S, Mazzaferro V, et al. Sorafenib in advanced hepatocellular carcinoma. N Engl J Med 2008;359(4):378–390.
8. Cheng AL, Kang YK, Chen Z, et al. Efficacy and safety of sorafenib in patients in the Asia-Pacific region with advanced hepatocellular carcinoma: a phase III randomised, double-blind, placebo-controlled trial. Lancet Oncol 2009;10(1):25–34.
9. Liu L, Cao Y, Chen C, et al. Sorafenib blocks the RAF/MEK/ERK pathway, inhibits tumor angiogenesis, and induces tumor cell apoptosis in hepatocellular carcinoma model PLC/PRF/5. Cancer Res 2006;66(24):11851–11858.
10. Adnane L, Trail PA, Taylor I, Wilhelm SM. Sorafenib (BAY 43-9006, Nexavar), a dual-action inhibitor that targets RAF/MEK/ERK pathway in tumor cells and tyrosine kinases VEGFR/PDGFR in tumor vasculature. Methods Enzymol 2006;407:597–612.
11. Guo Y, Klein R, Omary RA, Yang GY, Larson AC. Highly malignant intra-hepatic metastatic hepatocellular carcinoma in rats. Am J Transl Res 2010;3(1):114–120.
12. Deschamps F, Harris KR, Moine L, et al. Pickering-emulsion for liver transarterial chemo-embolization with oxaliplatin. Cardiovasc Intervent Radiol 2018;41(5):781–788.
13. Liang YJ, Yu H, Feng G, et al. High-performance poly(lactic-co-glycolic acid)-magnetic microspheres prepared by rotating membrane emulsification for transcatheter arterial embolization and magnetic ablation in VX2 liver tumors. ACS Appl Mater Interfaces 2017;9(50):43478–43489.
14. Tsai MJ, Lin MW, Huang YB, Kuo YM, Tsai YH. The influence of acute hyperglycemia in an animal model of lacunar stroke that is induced by artificial particle embolization. Int J Med Sci 2016;13(5):347–356.
15. Singh G, Chan H, Baskin A, et al. Self-assembly of magnetite nanocubes into helical superstructures. Science 2014;345(6201):1149–1153.
16. Kovalenko MV, Bodnarchuk MI, Lechner RT, Hesser G, Schäffler F, Heiss W. Fatty acid salts as stabilizers in size- and shape-controlled nanocrystal synthesis: the case of inverse spinel iron oxide. J Am Chem Soc 2007;129(20):6352–6353.
17. Park J, An K, Hwang Y, et al. Ultra-large-scale syntheses of monodisperse nanocrystals. Nat Mater 2004;3(12):891–895.
18. Chen J, White SB, Harris KR, et al. Poly(lactide-co-glycolide) microspheres for MRI-monitored delivery of sorafenib in a rabbit VX2 model. Biomaterials 2015;61:299–306.
19. Chen J, Sheu AY, Li W, et al. Poly(lactide-co-glycolide) microspheres for MRI-monitored transcatheter delivery of sorafenib to liver tumors. J Control Release 2014;184:10–17.
20. Park W, Chen J, Cho S, et al. Acidic pH-triggered drug-eluting nanocomposites for magnetic resonance imaging-monitored intra-arterial drug delivery to hepatocellular carcinoma. ACS Appl Mater Interfaces 2016;8(20):12711–12719.
21. Blanchet B, Billemont B, Cramard J, et al. Validation of an HPLC-UV method for sorafenib determination in human plasma and application to cancer patients in routine clinical practice. J Pharm Biomed Anal 2009;49(4):1109–1114.
22. Sheu AY, Zhang Z, Omary RA, Larson AC. Invasive catheterization of the hepatic artery for preclinical investigation of liver-directed therapies in rodent models of liver cancer. Am J Transl Res 2013;5(3):269–278.
23. Kim DH, Chen J, Omary RA, Larson AC. MRI visible drug eluting magnetic microspheres for transcatheter intra-arterial delivery to liver tumors. Theranostics 2015;5(5):477–488.
24. Kettenbach J, Stadler A, Katzler IV, et al. Drug-loaded microspheres for the treatment of liver cancer: review of current results. Cardiovasc Intervent Radiol 2008;31(3):468–476.
25. Ng R, Chen EX. Sorafenib (BAY 43-9006): review of clinical development. Curr Clin Pharmacol 2006;1(3):223–228.
26. Meyer T, Fox R, Ma YT, et al. Sorafenib in combination with transarterial chemoembolisation in patients with unresectable hepatocellular carcinoma (TACE 2): a randomised placebo-controlled, double-blind, phase 3 trial. Lancet Gastroenterol Hepatol 2017;2(8):565–575.
27. Lencioni R, de Baere T, Soulen MC, Rilling WS, Geschwind JFH. Lipiodol transarterial chemoembolization for hepatocellular carcinoma: a systematic review of efficacy and safety data. Hepatology 2016;64(1):106–116.
28. Kalayci C, Johnson PJ, Raby N, Metivier EM, Williams R. Intraarterial adriamycin and lipiodol for inoperable hepatocellular carcinoma: a comparison with intravenous adriamycin. J Hepatol 1990;11(3):349–353.
29. Johnson PJ, Kalayci C, Dobbs N, et al. Pharmacokinetics and toxicity of intraarterial adriamycin for hepatocellular carcinoma: effect of coadministration of lipiodol. J Hepatol 1991;13(1):120–127.

30. Choi JW, Cho HJ, Park JH, et al. Comparison of drug release and pharmacokinetics after transarterial chemoembolization using diverse lipiodol emulsions and drug-eluting beads. PLoS One 2014;9(12):e115898.
31. Idée JM, Guiu B. Use of Lipiodol as a drug-delivery system for transcatheter arterial chemoembolization of hepatocellular carcinoma: a review. Crit Rev Oncol Hematol 2013;88(3):530–549.
32. Vaidya S, Tozer KR, Chen J. An overview of embolic agents. Semin Intervent Radiol 2008;25(3):204–215.
33. Ford Versypt AN, Pack DW, Braatz RD. Mathematical modeling of drug delivery from autocatalytically degradable PLGA microspheres: a review. J Control Release 2013;165(1):29–37.
34. Buijs M, Geschwind JFH, Syed LH, et al. Spontaneous tumor regression in a syngeneic rat model of liver cancer: implications for survival studies. J Vasc Interv Radiol 2012;23(12):1685–1691.
35. Park W, Gordon AC, Cho S, et al. Immunomodulatory magnetic microspheres for augmenting tumor-specific infiltration of natural killer (NK) cells. ACS Appl Mater Interfaces 2017;9(16):13819–13824.
36. Nickerson MM, Song J, Shuptrine CW, Wieghaus KA, Botchwey EA, Price RJ. Influence of poly(d,l-lactic-co-glycolic acid) microsphere degradation on arteriolar remodeling in the mouse dorsal skinfold window chamber. J Biomed Mater Res A 2009;91(2):317–323.